LCOE Design Optimization Using Genetic Algorithm with Improved Component Models for Medium-Voltage Transformerless PV Inverters

Kyle J. Goodrick[†], Gab-Su Seo[*], Satyaki Mukherjee[†], Jinia Roy[*], Rahul Mallik[‡], Branko Majmunovic[†], Soham Dutta[‡], Dragan Maksimović[†], and Brian Johnson[‡]
[†]Colorado Power Electronics Center, Department of Electrical, Computer and Energy Engineering
University of Colorado, Boulder, CO 80309, USA
Email: {kyle.goodrick, satyaki.mukherjee, branko.majmunovic, maksimov}@colorado.edu
[*]Power Systems Engineering Center, National Renewable Energy Laboratory, Golden, CO 80401, USA
Email: {Gabsu.Seo, jinia.roy}@nrel.gov
[‡]Department of Electrical and Computer Engineering, University of Washington, Seattle, WA 98195, USA
Email: {rmallik, sdutta, brianbj}@uw.edu

***Abstract*—For real-world installations of photovoltaic and other renewable energy resources, the critical design metric is the levelized cost of energy (LCOE); however, many power electronics design optimizations are performed with efficiency and power density as the primary design goals. Recent work has shown that a new LCOE-focused optimization approach can yield improved system designs balancing cost and energy generation. This paper expands the LCOE optimization approach by considering comprehensive optimization parameters, adding new modeling of inductor cost, extending the semiconductor model to include effects of losses on housing cost, and implementing a genetic algorithm to improve computation efficiency.**

I. Introduction

Photovoltaic (PV) resources are becoming increasingly common in utility, commercial, and residential generation scenarios. Recent reports show that new installations of PV have increased by an order of magnitude over the last decade [1]. In order to compare the cost for various methods of solar generation and other sources of energy, a commonly used metric is the Levelized Cost of Energy (LCOE) [2].

As cost is a significant factor when installing new PV generation, reducing the LCOE is a high priority when designing PV systems. Recent work has shown that an LCOE improvement model can be used to evaluate the relative improvement in LCOE for a given topology [3]:

$$\frac{\Delta LCOE}{\overline{LCOE}} \approx \frac{\Delta C_0}{\bar{E}_{\text{life}}\overline{LCOE}} + \frac{\Delta\gamma}{\bar{\gamma}} \tag{1}$$

This work was authored in part by the National Renewable Energy Laboratory, operated by Alliance for Sustainable Energy, LLC, for the U.S. Department of Energy (DOE) under Contract No. DE-AC36-08GO28308. Funding was provided by the U.S. Department of Energy Office of Energy Efficiency and Renewable Energy (EERE) under Solar Energy Technologies Office (SETO), Agreement Number EE0008346. The views expressed in the article do not necessarily represent the views of the DOE or the U.S. Government.

where ΔLCOE is LCOE improvement of a new system from the baseline, $\overline{\text{LCOE}}$ is baseline LCOE, ΔC_0 is cost improvement, $\bar{E}_{\text{life}}$ is the total baseline energy generated during the system lifetime, and $\Delta\gamma$ and $\bar{\gamma}$ are improvement and baseline values for the power conversion efficiency scaling factor γ. This methodology allows various converter topologies to be compared without a full calculation of the LCOE for each one by assuming that only the elements changed will have an effect on the LCOE.

One topology of particular interest, the C^2 block architecture shown in Fig. 1, is described in [4] and the LCOE improvement offered by this topology is explored in [3]. In order to create a tractable design problem, [3] simplifies the design space by neglecting, linking, or constraining certain design variables based on engineering intuition of the architecture. In this paper, many of these simplifications are removed and the modeling is enhanced to more accurately determine the optimal system. As [3] uses a brute-force parameter sweep to find the optimal parameters, the computation time increases exponentially as new variables are added and as the parameter sweep becomes finer. Therefore, a different solving strategy must be employed if a finer sweep or more variables are desired. This paper uses a genetic algorithm, which is an optimization method that aims to replicate evolutionary processes [5]. The model extensions together with the genetic algorithm yield an advanced optimization process which more accurately determines optimal design values to minimize system LCOE.

II. Comprehensive Optimization Design Variables

In [3], three key design parameters: number of C^2 modules, on-resistance for dual-active bridge (DAB) primary-side switches, and core volume for both transformer and inductor are optimized. To reduce the computation burden in the brute-force method, other design parameters are deterministically computed from the three free variables. For instance, DAB

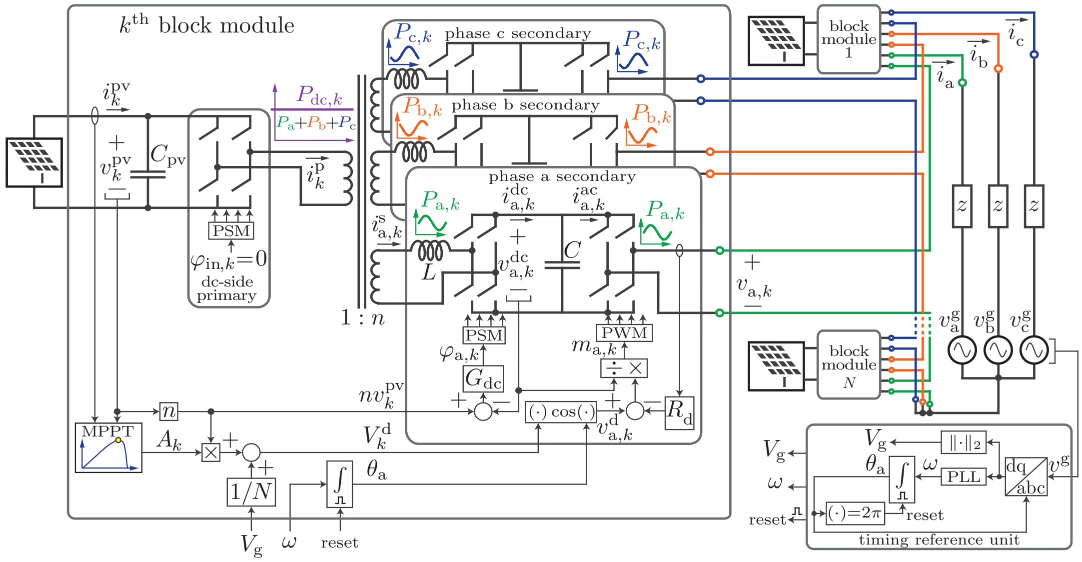

Fig. 1. C^2 building block circuit diagram and its control [4].

secondary-side and inverter switches are scaled based on their rms current relative to the primary side. In addition, switching frequency for both the DABs and the inverter were assumed to be fixed; however, both of these variables can have a significant impact on the size of passive components and the efficiency and, as a result, both affect the LCOE. This work also fully evaluates semiconductor design. In [3], switch on-resistances are scaled with respect to the primary side value based on intuition that balancing the conduction loss on each switch may yield the optimum; however, this may not be valid for all operating modes as it does not consider switching losses. To fill this gap, this paper frees all three variables to be adjusted individually. This paper also decouples the inductor size from the transformer allowing the varying impact of the two components sizes to be fully evaluated.

III. Semiconductor Model

A. Review of Semiconductor Model

The semiconductor model developed in [3] is capable of predicting the approximate output capacitance of a MOSFET given an on-resistance and a blocking voltage. To develop a comprehensive, scalable model, SiC MOSFET switch data available publicly from Cree [6] is used in this paper. These datasheets provide not only the on-resistance, blocking voltage, and output capacitance, but also contain the die area of the MOSFET. With this data, we can calculate the specific on-resistance of the device, $R_{ds,sp}$, as a function of blocking voltage with

$$R_{ds,sp} = K_{SiC} V_{BD}^{\kappa} \tag{2}$$

where κ and K_{SiC} can be estimated using the Cree data. Both parameters physically depend on material properties and process specifics [7]. The output capacitance can then be modeled as a parallel plate capacitor whose properties depend on blocking voltage and on-resistance connected in parallel with a fixed capacitance, as shown in (3) and (4).

$$C_{oss} = \epsilon \frac{A_{die}}{W_d} + C_{fixed} \tag{3}$$

$$W_d = 2 \frac{V_{BD}}{E_{C,SiC}} \tag{4}$$

B. Semiconductor Model Extensions

One factor that is neglected in [3] is the effect that the semiconductor losses have on the thermal performance required by the system and the associated costs. To account for this, an extension to the model was developed. The model works in a fashion that is similar to those for calculating costs in [3]. First the cost associated with the housing in the baseline inverter is calculated by multiplying the levelized cost of the baseline converter [8] with the relative cost of the housing [9]. This forms the constant baseline LCOE for the housing. To determine the levelized cost of a given converter, the required thermal impedance is calculated using a thermal model that takes into account the peak operating temperature of SiC and the fixed die to case thermal impedance of a typical device. The LCOE for the housing is then calculated using the relative thermal cost model described in [9] and the levelized cost from [8]. The LCOE improvement can then be calculated with the previous two results.

IV. Magnetics Model Extensions

An additional effect that was neglected in [3] was the cost of the inductor. It was assumed that the cost would be comparable to any inductors in baseline inverter and would therefore have a negligible effect on the LCOE. However, the inductor required in the DAB is quite small as it is only an AC inductor and must not carry DC current, so cost reductions are likely. To extend the model to account for these effects, a procedure similar to that performed in the semiconductor model is employed.

First a baseline value for inductor cost is calculated by taking the levelized value for inverter cost in [8] and multiplying it by the relative cost of the magnetics in the baseline converter [9]. The cost for a given system's inductor is calculated using the cost model in [3] which maps core volume to levelized cost. The LCOE improvement is then calculated by the difference between the baseline value and the given value.

V. Model Summary

As shown in (1) the LCOE improvement for a system may be computed with baseline values for the LCOE ($\overline{LCOE}$), lifetime system energy ($\bar{E}_{\text{life}}$), and power conversion efficiency ($\bar{\gamma}$) as well as values representing the changes in cost (ΔC_0) and efficiency ($\Delta\gamma$) for the new system. With the model extensions discussed in this paper ΔC_0 can be computed with

$$\begin{aligned}\Delta C_0 &= \Delta C_{0,\text{trans}} + \Delta C_{0,\text{ind}} + \Delta C_{0,\text{semi}} + \Delta C_{0,\text{house}} \\ &= (C_{\text{trans,bench}} - C_{\text{trans},C^2}) + (C_{\text{ind,bench}} - C_{\text{ind},C^2}) \\ &+ (C_{\text{semi,bench}} - C_{\text{semi},C^2}) + (C_{\text{house,bench}} - C_{\text{house},C^2})\end{aligned} \tag{5}$$

where $\Delta C_{0,\text{trans}}$ and $\Delta C_{0,\text{ind}}$ are the cost improvements by employing high frequency magnetics instead of low frequency transformers, and $\Delta C_{0,\text{semi}}$ and $\Delta C_{0,\text{house}}$ are the improvement in semiconductor and housing cost from baseline. Additionally, $\Delta\gamma$ may be computed with

$$\Delta\gamma = \gamma - \bar{\gamma} = c_t(\eta_{\text{PC},C^2} - \eta_{\text{PC,bench}}) \tag{6}$$

where c_t is the capacity factor of a PV system depending on geographical location, and η_{PC}, C^2 and $\eta_{\text{PC,bench}}$ are efficiency of C^2 and benchmark system, respectively as defined in [3].

VI. LCOE Optimization using a Genetic Algorithm

With the variables swept in [3], the script runs in approximately three minutes. As additional variables are added, the computation time increases by a factor equal to the number of steps in sweeps of the new variable values. As discussed in Section II this paper is adding five additional variables to the design space. In [3] each variable has at least nine steps. Using the same number of steps for the new variables would increase the run time to more than four months. It is therefore necessary to use a less computationally intensive optimization algorithm.

Many optimization techniques are possible for the nonlinear problems encountered in power electronics, including geometric programming (GP) [10], [11], particle swarms [12], and genetic algorithms [13]–[16]. GP is the most computationally efficient method, but it requires extensive work up front to model the problem in GP compatible expressions and necessitates simplification of the system model. Genetic algorithms and particle swarm algorithms are particularly attractive because they do not require modifications or simplifications to the model. In this work, a genetic algorithm is implemented using MATLAB's global optimization toolbox. Fig. 2 illustrates

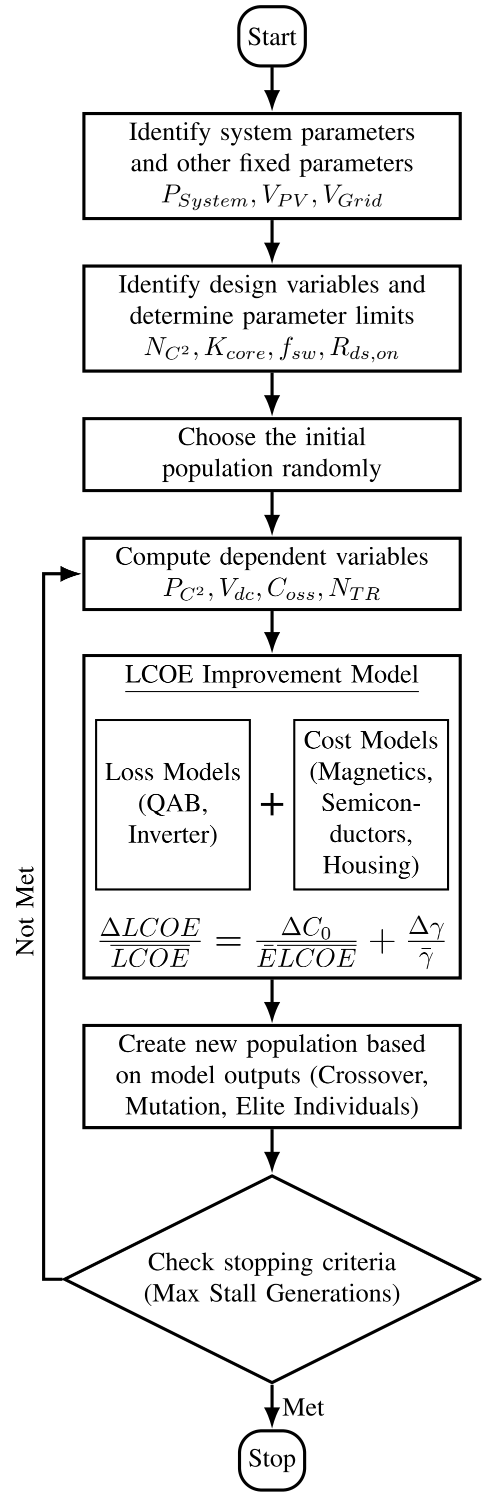

Fig. 2. Genetic Algorithm Flow Chart

TABLE I
OPTIMIZATION PROBLEM VARIABLES

Type	Variable	Symbol
Inputs	System Power	P_{System}
	PV Panel Voltage	V_{PV}
	Grid Voltage	V_{Grid}
Design	Number of C^2 Modules	N_{C^2}
	Transformer Volume	V_{tr}
	Inductor Volume	V_{ind}
	Primary Switch On Resistance	$R_{ds,pri}$
	Secondary Switch On Resistance	$R_{ds,sec}$
	Inverter Switch On Resistance	$R_{ds,inv}$
	DAB Switching Frequency	$f_{sw,dab}$
	Inverter Switching Frequency	$f_{sw,inv}$
Outputs	Change in LCOE	$\Delta LCOE$

the optimization method and Table I shows the variables in the optimization procedure. Different from the brute-force method, it determines the next population based on the model outputs which accelerates the optimization process and does not require discrete variable values.

While many of the genetic algorithm's settings are standard there are a few noteworthy exceptions. Firstly, the genetic algorithm is modified to be a mixed integer design problem by limiting the values of the number of modules to integers. The second change is the addition of a non-linear constraint function on the design variables and finally an initial population is generated in a non-standard way to ensure switching frequencies are distributed logarithmically.

A. Nonlinear Constraint Function

The nonlinear constraint prevents the solver from choosing a core volume that is too small to fit the number of turns required to prevent saturation of the transformer. To verify that a given core volume is large enough the inequality

$$d_w \geq 2d_e + d_{cu} N_{tr}\, \mathrm{ceil}(N_{\min}/m_{\max}) \tag{7}$$

must be satisfied. Where d_w is the width of the winding window and can be calculated with

$$d_w = W_{core,base} \sqrt[3]{K_{core,vol}}\,, \tag{8}$$

where $W_{core,base}$ is the core winding window width when $K_{core,vol}$ is 1 and $K_{core,vol}$ is the core volume scaling factor, $m_{\max}$ is the maximum number of PCB copper layers, d_e is the minimum copper-to-board-edge distance, $d_{cu} = d_{tr} + d_{sep}$ where d_{tr} is the minimum trace width and d_{sep} is the minimum trace spacing, N_{tr} is the turns ratio of the transformer and can be calculated with

$$N_{tr} = \mathrm{ceil}\left(\frac{V_{grid,pk,C^2} V_{dc,Scale}}{V_{pv}}\right) \tag{9}$$

where $V_{dc,Scale}$ is a constant term that gives the system margin between the required and actual DC bus voltage, V_{pv} is the nominal PV panel voltage, and V_{grid,pk,C^2} is the peak line-to-neutral AC voltage that must be produced by each C^2 module which can be calculated with

$$V_{grid,pk,C^2} = \frac{V_{grid,pk}}{N_{C^2}} \tag{10}$$

where N_{C^2} is the number of modules and $V_{grid,pk}$ is the peak voltage that the system must produce which can be calculated with

$$V_{grid,pk} = V_{grid}\sqrt{\frac{2}{3}} \tag{11}$$

where V_{grid} is the line-to-line nominal grid voltage of the system, and $N_{\min}$ is the minimum number of turns to prevent saturation and can be calculated with

$$N_{\min} = \frac{\lambda}{A_W B_{\max}} \tag{12}$$

where

$$\lambda = \frac{V_{pv}}{2 f_{sw,dab}} \tag{13}$$

and

$$A_W = A_{W,base} K_{core,vol}^{2/3}\,. \tag{14}$$

In Eqs. (12) to (14) λ is the flux linkage of the transformer, $B_{\max}$ is the maximum allowable flux density, $f_{sw,dab}$ is the switching frequency of the DAB, A_W is the cross sectional area of the core, and $A_{W,base}$ is the area of the core when $K_{core,vol}$ is 1. Finally the inequality is put into the form

$$0 \geq 2d_e + d_{cu} N_{tr}\, \mathrm{ceil}(N_{\min}/m_{\max}) - d_w\,, \tag{15}$$

which is required for the MATLAB GA solver.

B. Initial Population Distribution

To start the genetic algorithm and initial population must be generated randomly. For continuous variables that do not have any special considerations this can be done with

$$V_{gene} = B_l + (B_u - B_l)\,\mathrm{rand}(N) \tag{16}$$

where V_{gene} is an array of gene values for each member of the population for a given gene, B_l is a lower boundary on the gene's value, B_u is an upper boundary, N is the size of the population, and rand is a function that returns an array of the size of the argument containing random numbers between 0 and 1. However, this will cause problems in two cases for this optimization problem. The first is with the number of modules, which must be an integer. This may be solved by modification of the gene value generation function to

$$V_{gene} = \mathrm{floor}(B_l + (B_u - B_l + 1)\,\mathrm{rand}(N))\,. \tag{17}$$

Finally, the function must be modified for the two switching frequencies optimized in the problem. As the switching frequency bounds cover several orders of magnitude, it is necessary for their distribution to be logarithmic to ensure that the points are evenly distributed across each order of magnitude. For these genes

$$V_{gene} = 10^{\log(B_l) + (\log(B_u) - \log(B_l))\,\mathrm{rand}(N)} \tag{18}$$

is used to generate the population's initial values.

TABLE II
OPTIMAL DESIGN PARAMETERS

N_{C^2}	V_{tr} [cm^3]	V_{ind} [cm^3]	$R_{ds,pri}$ [mΩ]	$R_{ds,sec}$ [mΩ]	$R_{ds,inv}$ [mΩ]	$f_{sw,dab}$ [kHz]	$f_{sw,inv}$ [kHz]
15	484	265	96.5	323	159	75	32

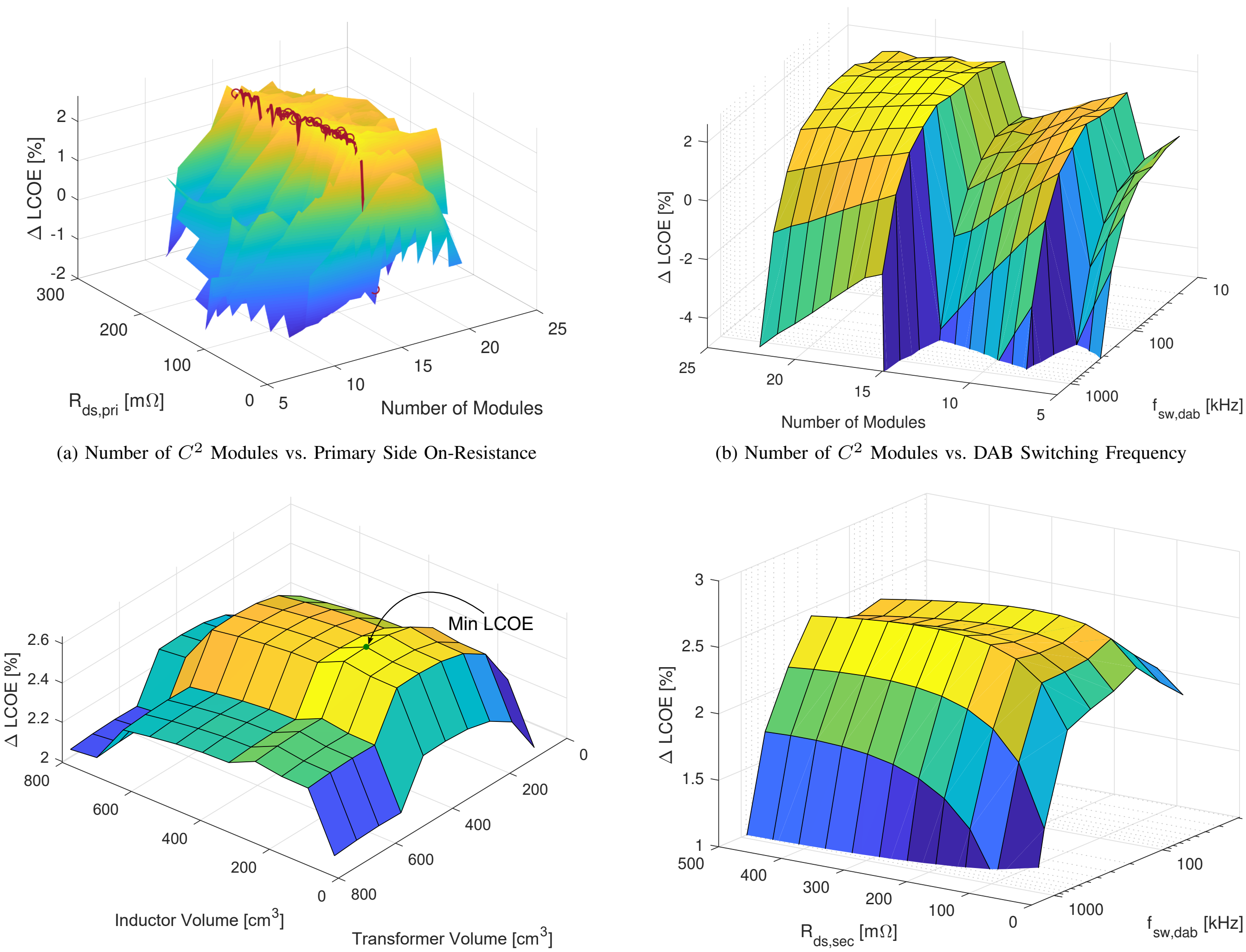

(a) Number of C^2 Modules vs. Primary Side On-Resistance

(b) Number of C^2 Modules vs. DAB Switching Frequency

(c) Inductor Volume vs. Transformer Volume

(d) Secondary Side On-Resistance vs. DAB Switching Frequency

Fig. 3. Surface plots showing the relationships between various parameters and the LCOE improvement. The red line in (a) shows the path taken by the best design for each generation and the circles represent the best value for each generation. (a) is plotted with data from the genetic algorithm and (b) - (d) are plotted with sweeps around the optimal value to hold the variables not plotted constant.

VII. Results and Discussion

With the improved device and system models and the optimization method with the customized setup, the same baseline values including baseline cost and efficiency derived in [3] are used to assess improvement from the work. In the same manner, 2018 LCOE benchmark data reported in [8] is employed. With the new models and variables, the genetic algorithm yields an optimal solution with an LCOE improvement of 2.61 %, which represents an LCOE improvement factor 30 % greater than reported in [3] for a 200 kW PV generation system. All optimal design variables found in the optimization are tabulated in Table II. Several surface plots of the complete population are shown in Fig. 3. Of particular interest, Fig. 3a shows that the number of modules is a critical parameter in the optimization. There is a steep rise in the LCOE improvement at 15 modules, which corresponds with the point where each module no longer needs a 1:2 turns ratio transformer to create the medium voltage output. At this point, only a 1:1 turns ratio is needed, and the DAB secondary-side and inverter switches voltage rating may change from

2400 V devices to 1200 V devices which are considerably cheaper and result in less switching losses, i.e., better figure of merit. Fig. 3b displays the interplay of number of C^2 modules and switching frequency. As expected in Section II, switching frequency is a key driving factor for LCOE improvement. Fig. 3c shows the impact of magnetic sizes on the LCOE and how decoupling the transformer and inductor designs leads to better optimization. Fig. 3d illustrates relationship between optimal on-resistance and switching frequency. Additionally, as noted in Section II, different optimal switch designs are found to also depend on switching losses and, as seen in Table II, the optimal switch ratios are different than those predicted by the rms current ratio as in [3] illustrating the importance of freeing these variables.

As shown in the results, by adding and incorporating decoupled variables, the advanced optimization method can find better design values without significant computational burden and provide more design insights.

VIII. Conclusion

This paper has presented an advanced modeling and LCOE optimization process for a PV generation system using the C^2 modular architecture. It expands the optimization procedure to include new variables, new models, and develops a genetic algorithm to efficiently find the optimal point in the expanded design space. The advanced optimization incorporating the comprehensive model can provide engineering insights of the new power electronics architecture and determine optimal design values for the key components with manageable computational efficiency. For a 200 kW PV system example, the method results in an LCOE improvement of more than 2.6 %, a 30 % increase over the previous results for the same system with limited free variables.

References

[1] BloombergNEF, "Annual Global PV New Build," Bloomberg Professional service, Tech. Rep., Jul. 2019.

[2] K. Branker, M. J. M. Pathak, and J. M. Pearce, "A review of solar photovoltaic levelized cost of electricity," *Renewable and Sustainable Energy Reviews*, vol. 15, no. 9, pp. 4470–4482, Dec. 2011.

[3] G. Seo, S. Mukherjee, J. Roy, K. Goodrick, R. Mallik, B. Majmunovic, S. Dutta, D. Maksimovic, and B. Johnson, "Levelized-Cost-of-Electricity-Driven Design Optimization for Medium-Voltage Transformerless Photovoltaic Converters," in *Energy Conversion Congress and Exposition (ECCE)*. Baltimore, Md., United States: IEEE, Sep. 2019.

[4] P. K. Achanta, B. B. Johnson, G. Seo, and D. Maksimovic, "A Multilevel DC to Three-Phase AC Architecture for Photovoltaic Power Plants," *IEEE Transactions on Energy Conversion*, vol. 34, no. 1, pp. 181–190, Mar. 2019.

[5] D. Whitley, "A genetic algorithm tutorial," *Statistics and Computing*, vol. 4, no. 2, pp. 65–85, Jun. 1994.

[6] C. Wolfspeed, "Silicon Carbide Power MOSFET Datasheets," Jan. 2016.

[7] N. Mohan, *Power Electronics : Converters, Applications, and Design*, 3rd ed. Hoboken, NJ: John Wiley & Sons, 2003.

[8] R. Fu, D. Feldman, and R. Margolis, "U.S. Solar Photovoltaic System Cost Benchmark: Q1 2018," National Renewable Energy Laboratory, Golden, CO, Tech. Rep. NREL/TP-6A20-72399, 2018.

[9] U. Schwarzer, S. Buschhorn, and K. Vogel, "System Benefits for Solar Inverters using SiC Semiconductor Modules," in *PCIM Europe 2014; International Exhibition and Conference for Power Electronics, Intelligent Motion, Renewable Energy and Energy Management*, May 2014, pp. 1–8.

[10] A. Stupar, T. McRae, N. Vukadinovic, A. Prodic, and J. A. Taylor, "Multi-Objective Optimization of Multi-Level DC-DC Converters using Geometric Programming," *IEEE Transactions on Power Electronics*, pp. 1–1, 2019.

[11] R. A. Jabr, "Application of geometric programming to transformer design," *IEEE Transactions on Magnetics*, vol. 41, no. 11, pp. 4261–4269, Nov. 2005.

[12] S. E. D. León-Aldaco, H. Calleja, and J. A. Alquicira, "Metaheuristic Optimization Methods Applied to Power Converters: A Review," *IEEE Transactions on Power Electronics*, vol. 30, no. 12, pp. 6791–6803, Dec. 2015.

[13] M. Liserre, A. Dell'Aquila, and F. Blaabjerg, "Genetic algorithm-based design of the active damping for an LCL-filter three-phase active rectifier," *IEEE Transactions on Power Electronics*, vol. 19, no. 1, pp. 76–86, Jan. 2004.

[14] B. Ozpineci, L. M. Tolbert, and J. N. Chiasson, "Harmonic optimization of multilevel converters using genetic algorithms," *IEEE Power Electronics Letters*, vol. 3, no. 3, pp. 92–95, Sep. 2005.

[15] A. Garcia-Bediaga, I. Villar, A. Rujas, L. Mir, and A. Rufer, "Multi-objective Optimization of Medium-Frequency Transformers for Isolated Soft-Switching Converters Using a Genetic Algorithm," *IEEE Transactions on Power Electronics*, vol. 32, no. 4, pp. 2995–3006, Apr. 2017.

[16] D. V. Malyna, J. L. Duarte, M. A. M. Hendrix, and F. B. M. van Horck, "Optimization of combined thermal and electrical behavior of power converters using multi-objective genetic algorithms," in *2007 European Conference on Power Electronics and Applications*, Sep. 2007, pp. 1–10.